

Learning Only What Valid Adapters Can Express: Subspace-Constrained Adaptation Against Fine-Tuning Poisoning

Fabien Polly*

July 2026

Abstract

Parameter-efficient fine-tuning still leaves a broad space of behavior-changing updates reachable, so a poisoned objective can be represented and optimized. We study an alternative: adaptation constrained to the subspace estimated from a trusted pool of existing task adapters. On `flan-t5-large` with 196 public LoRA adapters, we show that (1) the functionally relevant content of an adapter lies in a low-dimensional shared subspace, 30 to 38 percent of its weight norm being redundant under the evaluated task distributions; (2) gradient adaptation restricted to 128 coordinates on this subspace matches full LoRA fine-tuning on clean classification data, while under targeted label inversion LoRA collapses to 3–26 percent exact match and the constrained learner keeps 62–96 percent on the tasks the pool covers; (3) the constrained learner cannot fit corrupted data, its adaptation loss separating clean from garbage by two orders of magnitude ($120\times$), an out-of-distribution signal for free; and (4) against an adaptive backdoor attacker who optimizes within the subspace, the attack is blocked (8 percent success versus 100 for LoRA) on the task where its target behavior is unlike anything in the pool, and only partially blocked (85 percent) when the target coincides with a common pool behavior. On these two tasks the outcome is consistent with how close the target is to the pool’s directions, which suggests but does not establish a pool-relative boundary. The mechanism trades peak plasticity for these properties: on tasks the pool covers poorly, unconstrained fine-tuning wins, and the guarantee assumes the pool itself is trusted. Code and data are public.

1 Introduction

Fine-tuning is an attack surface. A consumer medical assistant maliciously personalized to recommend a dangerous dose, a corporate model taught by a poisoned document to exfiltrate its database on a trigger word, a brand chatbot absorbing toxic user chats, a model fine-tuned on scraped web text that a coordinated edit campaign has seeded with falsehoods: every adaptation on data the operator does not fully control is a vulnerability. A few hundred corrupted instructions suffice to compromise an aligned model [12, 8]. Existing defenses inspect the data (filtering, influence functions) or dampen the update (regularization); all are heuristic in the sense that a successful attack remains expressible, the defense just makes it harder to reach.

We study a defense that shrinks expressibility instead. The weight updates a model acquires when learning legitimate tasks do not fill update space; they concentrate in a low-dimensional shared subspace. If adaptation is constrained to that subspace, the set of reachable updates is greatly reduced, and we find empirically that the poisoned objectives in our threat models require updates outside it: they cannot be fit, and that failure is visible in the training loss. We are careful not to overclaim: a subspace spanned by legitimate adapters can still contain far extrapolations and combinations unlike any single adapter, so this is empirical protection against the attacks we test, not a proof that no harmful behavior is expressible (Section 5).

We instantiate the idea with the affine span of a public pool of LoRA adapters, and evaluate it on a real language model against an equal-data, equal-optimization-step LoRA baseline. Our contributions: (1) an analysis of the functional geometry of 196 public adapters showing that 30 to 38 percent of an adapter’s weight norm is functionally redundant under the evaluated distributions; (2) a constrained adaptation mechanism

*Independent researcher. Code and data: <https://github.com/infinity/z-manifold>

with 128 trainable coordinates that matches LoRA fine-tuning on clean data; (3) a poisoning study showing an order-of-magnitude robustness gap under targeted label inversion; (4) a built-in out-of-distribution signal separating clean from garbage adaptation data by two orders of magnitude. Everything runs on one consumer GPU and all code, data, and seeds are public.

2 Related work

Latent adaptation. LEO [10] performs gradient descent on a latent code with a frozen decoder in its inner loop, for few-shot classification, decoding only a final linear layer; its headline pipeline adds weight-space fine-tuning after decoding, and no safety property is evaluated. Our test-time mechanism is LEO’s ablated z-only variant, applied to the LoRA deltas of a language model and evaluated for safety. **Feed-forward adapter generation.** Text-to-LoRA [3] and Drag-and-Drop LLMs [7] generate LoRA parameters in a single forward pass from task descriptions or prompts; neither performs test-time optimization nor evaluates poisoning, OOD detection, or forgetting. Text-to-LoRA’s appendix documents the weight-space misalignment of independently trained adapters that we also observe and work around by operating in ΔW space. **Adapter subspaces (closest work).** EigenLoRAx [6] recycles existing adapters into a principal subspace and adapts new tasks by learning only coefficients within it, for efficiency; the mechanism is close to ours. Compress-then-Serve [2] learns shared bases over many LoRAs for serving, and LoraHub [5] composes adapters for cross-task generalization. Our mechanism (optimize coefficients in an adapter subspace) is not the contribution; these works already establish that new tasks can be adapted inside such a subspace. Our contribution is to use the subspace as an *expressivity barrier against poisoning* and to show that the optimization residual is itself a rejection signal. In one line: EigenLoRAx is efficiency and recycling, LoraHub is composition, ours is safety by restriction of the reachable set plus detection by non-learnability. **Weight-space structure.** Model zoos [11] study populations of trained networks; permutation symmetry [1] explains why independently trained networks are misaligned in raw weight space, which motivates our use of the gauge-invariant ΔW representation. **Poisoning of fine-tuning.** Instruction tuning can be poisoned with a few hundred examples [12], and even benign fine-tuning degrades safety alignment [8]. These works motivate the threat model; existing mitigations are data-side (filtering, provenance) or update-side (regularization, constrained norms), all leaving the attack expressible. We instead make the attack geometrically unreachable.

3 Method

Pool of n adapters with deltas $\Delta W_j = B_j A_j$ (gauge invariant; we never compare raw (A, B) factors). Frobenius inner products are computed in factored form, $\langle \Delta W_i, \Delta W_j \rangle = \text{tr}((B_i^\top B_j)(A_j A_i^\top))$, giving a Gram matrix $G \in \mathbb{R}^{n \times n}$ without materializing any ΔW .

Basis. For a held-out task i we take the other $n-1$ adapters, double-center their Gram submatrix, and compute its eigendecomposition; the top K eigenvectors give an orthonormal basis of the pool’s span, expressed as coefficient vectors over the adapters. This is a full $(n-1) \times (n-1)$ eigendecomposition recomputed per held-out task; with $n = 196$ it costs a few milliseconds and is exact, not an approximation or a rank-one update. Because the pool of task i excludes i , the target adapter is never in its own basis, which prevents leakage in the reconstruction experiments (Section 4.2).

Adaptation. We optimize a code $z \in \mathbb{R}^K$ and set $\Delta W(z) = \sum_j g_j(z) \Delta W_j$ with the mixing weights $g(z) = Mz + b$ affine in z : $M \in \mathbb{R}^{n \times K}$ carries the basis eigenvectors scaled by the empirical per-component standard deviation, and b is the pool-mean weight, so $z = 0$ (its initialization) decodes to the mean adapter. Only z is trained by gradient descent; the base model and the pool are frozen. In this base method the reachable set $\{\Delta W(z)\}$ is therefore the affine span of the pool. The implementation wraps the q and v projections with stacked factor matrices; the overhead is about $3 \times$ a forward pass on the wrapped projections and no basis is ever materialized. Section 4.6 replaces the affine g with a nonlinear generator to test whether a curved manifold helps.

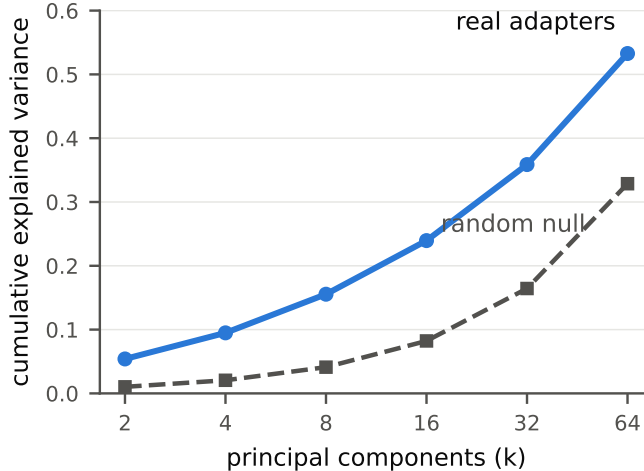


Figure 1: Cumulative explained variance of the 196 adapters in ΔW space versus a norm-matched random-LoRA null. Structure is real (top-32 captures 35.9% versus 16.4% for the null) but not naively low-dimensional (effective dimension 129 of 196). Within-family cosine similarity is 0.204 versus 0.018 across families.

4 Experiments

Setup: flan-t5-large (783M, bf16), 196 LoraHub adapters (rank 16, q and v , 144 modules, 9.4M parameters each), P3 tasks, 128 training examples per task, identical step budgets for both methods (8 epochs, batch 8), LoRA baseline freshly initialized with rank 16. Three seeds per cell. A 12 GB consumer GPU suffices.

4.1 Structure of the adapter pool

The effective dimension of 129 out of 196 is itself informative: the safety of the method does not come from crushing the model into a tiny subspace, but from removing precisely the directions no legitimate adapter uses. The constrained learner keeps most of the pool’s expressive capacity while excluding the rest.

4.2 Functional dimension

The spectrum measures geometry; here we ask how much of an adapter is functionally necessary. For a held-out adapter, we reconstruct it from the leave-one-out basis of the other 195: we keep the projection of its ΔW onto the top- k principal directions of the pool, apply that reconstruction to flan-t5-large, and read the validation cross-entropy per token on the adapter’s own task (Figure 2). We do this on the tasks where the original adapter measurably beats the base model, so that a change in accuracy is meaningful. The function is fully recovered at a modest rank, $k = 8$ for wiki_hop and $k = 128$ for amazon_polarity, even though 30 to 38 percent of the adapter’s weight norm lies outside the pool’s span and is thrown away in the reconstruction. That discarded component is orthogonal to every other adapter and carries no measurable function on the task; it is the degeneracy of independently trained low-rank updates, not signal. In other words, the part of an adapter that matters already lives in the shared subspace, which is what makes constraining adaptation to that subspace viable rather than crippling.

4.3 Poisoning

Under intra-task label shuffling (a weak poison preserving the label marginal), LoRA often resists through benign memorization; under targeted inversion the gap is an order of magnitude (Figure 3, Table 1). The prior is capped by pool quality: on tasks whose pool adapters are weak (race), LoRA reaches lower clean CE than constrained adaptation. This trade-off is inherent and we report it as such.

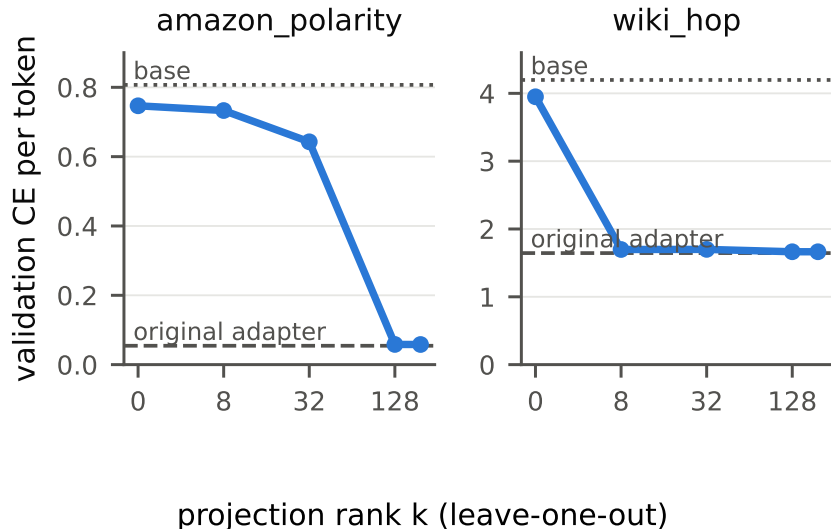


Figure 2: Validation cross-entropy of an adapter reconstructed by leave-one-out projection on the top- k principal directions of the other 195. Function is fully recovered at $k=8$ (wiki_hop) to $k=128$ (amazon_polarity) while 30 to 38 percent of the weight norm, orthogonal to the pool, is discarded with no functional cost.

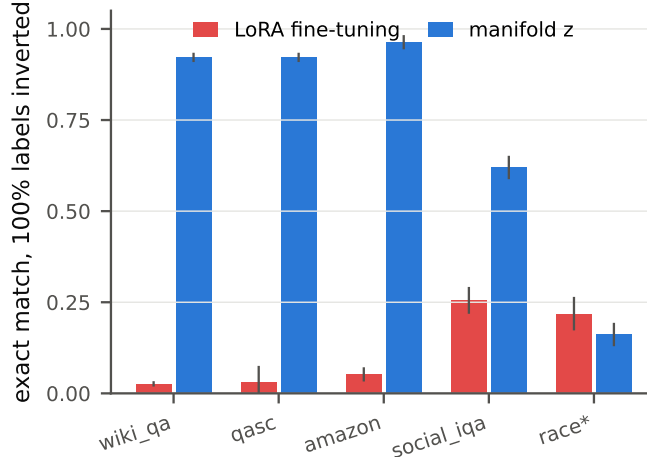
Table 1: Exact match on clean validation after adapting on 128 examples, mean \pm standard deviation over 3 seeds. Inversion replaces the targeted labels with guaranteed wrong ones. Bold marks the better method per cell. The first four tasks are within the pool’s reach; race is a task the pool covers poorly, where the constraint caps performance below LoRA even on clean data, though z stays flat under corruption while LoRA does not.

Task	clean		50% inverted		100% inverted	
	LoRA	z	LoRA	z	LoRA	z
wiki_qa	0.99	0.99	0.49	0.99	0.03	0.92
qasc	0.99	0.98	0.59	0.92	0.03	0.92
amazon	0.94	0.95	0.58	0.95	0.05	0.96
social_iqa	0.72	0.68	0.45	0.66	0.26	0.62
race (weak pool)	0.31	0.13	0.29	0.17	0.22	0.16

Why the poison is not expressible. A label-inverted task requires a weight update that maps each input to the opposite of its correct answer. No legitimate adapter in the pool implements such a mapping, so the update has a large component orthogonal to the pool’s span. Constrained adaptation can only realize the in-span projection of that update, which for a systematic inversion is close to the pool mean (a weak, non-inverting adapter); the inverting direction is simply unavailable. LoRA, unconstrained, follows the full update and learns the inversion faithfully. This is the mechanistic content of the gap in Table 1, and it predicts the failure mode we do observe: the method degrades gracefully toward a generic adapter rather than toward a harmful one.

4.4 Incompatibility signal (a pool-relative OOD detector)

The same mechanism that blocks the poison produces a detector: data the pool cannot express keeps the adaptation loss high. Thresholding the final adaptation loss separates clean from garbage with AUROC 1.0 for both methods on these samples, so detectability itself is not unique to our method. Two things are: the margin is two orders of magnitude for constrained adaptation versus one for LoRA, and for constrained adaptation a high loss *coincides* with safety (the poison was not learned), whereas LoRA reaches a low loss



* race: adapter pool covers this task poorly (see text)

Figure 3: Exact match on clean validation after adapting on 128 examples with 100 percent targeted label inversion, per task (mean and standard deviation over 3 seeds). On the four tasks the pool covers, constrained adaptation keeps 0.62 to 0.96 while LoRA collapses to 0.03 to 0.26. race is the weak-pool case (Table 1): both are low and the constraint does not help.

precisely by learning the poison. The detector is relative to the pool, which is a genuine caveat: a legitimate task far from everything in the pool would also plateau, a false positive. Sensitivity to poison and coverage of hard-but-legitimate tasks are two sides of the pool’s span; we therefore read the plateau as “outside the pool” rather than “adversarial” per se.

4.5 Sequential adaptation

We train one adapter continually over a chain of five tasks (three seeds, three chain orders) and measure both forgetting, the rise in a task’s validation CE between just after it was learned and the end of the chain, and recovery, re-learning the first task from 16 examples after the full chain. Averaged over seeds, constrained adaptation forgets slightly less than LoRA (0.40 versus 0.47 mean CE rise) and far more consistently (± 0.11 versus ± 0.41): LoRA forgets catastrophically on some chains (one task’s CE rising above 2.5), while the constraint bounds the damage. On the pool-covered tasks the gap is clear (Figure 5); race, again, is where the constraint hurts. Recovery is mixed and dominated by whichever task is first in the chain: it favors z when that task is pool-covered (0.06 versus 0.20 CE when amazon is first) and LoRA when it is race. We report the aggregate without overclaiming a recovery advantage.

4.6 Nonlinear generator versus PCA

Is the affine subspace of Section 3 leaving anything on the table? We compare, at equal code size, a linear PCA truncation and a small autoencoder trained on the other 195 adapters’ coordinates, reconstructing each held-out adapter and scoring its function. At bottleneck 32 the autoencoder beats PCA-32 on all five tasks (Figure 6), so the pool does have mild nonlinear structure that a curved generator captures. But PCA-64, a larger linear subspace, beats the nonlinear AE-32: nonlinearity buys code efficiency, not peak fidelity. We therefore keep the linear subspace as the main method for its simplicity and report the autoencoder as evidence that “manifold” is more than a figure of speech, without claiming the nonlinear generator is necessary.

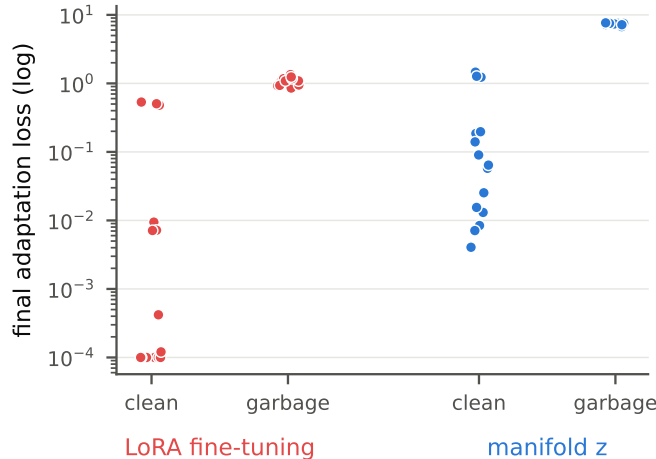


Figure 4: Final adaptation loss on clean versus garbage targets (log scale, one point per task and seed). Constrained adaptation cannot descend on garbage (median 7.4 versus 0.06 clean, a 120 \times margin); LoRA also separates but by a much smaller margin (1.0 versus 0.0) and, crucially, ships a corrupted model.

4.7 Controls: leakage and low-dimension

Two controls address the most natural objections. **Dataset-family holdout.** Our pool contains several adapters per source dataset (nine amazon_polarity prompts, nine wiki_qa, and so on), so leaving out only the target adapter still leaves near-siblings in the basis. We rebuild the basis excluding *every* adapter from the target’s dataset (4 to 9 removed per task) and re-run clean and 100% inversion. **Random subspace.** To separate the pool’s semantics from the mere fact of a 128-dimensional constraint, we replace the pool with 128 random rank-16 pseudo-adapters (Gaussian, Frobenius-norm-matched) and adapt in their span. Both controls come out as the mechanism predicts (Table 2). Removing every same-dataset sibling barely changes constrained adaptation: at 100% inversion it keeps 0.65 to 0.99 exact match (versus 0.62 to 0.96 with the full pool), while LoRA still collapses to 0.03 to 0.26. The robustness is therefore not a leakage artifact. The random subspace, by contrast, is useless: at equal size and budget it reaches only 0.06 to 0.53 exact match on *clean* data (versus 0.68 to 0.99 for the pool), so a 128-dimensional constraint alone buys neither utility nor meaningful robustness. What the pool provides, that a random subspace of the same size does not, is the combination of clean utility and poison resistance; low dimension alone gives neither.

A third control asks whether the protection is just slower learning. We run LoRA with strong regularization (weight decay 0.1 plus dropout 0.3, and weight decay 1.0). Both keep clean performance (0.94 to 0.99) and both still collapse under inversion (0.01 to 0.05 exact match on the first three tasks), identical to plain LoRA. A norm penalty does not restrict *which* solutions are reachable, only how fast they are reached, so it offers no poison resistance. The constraint is doing something a regularizer cannot.

A fourth control addresses an asymmetry in the comparison: constrained adaptation starts from $z = 0$, which decodes to the pool-mean adapter, a non-trivial prior, whereas LoRA starts from a near-zero update. One might worry that the poison resistance is just the method staying near a good starting point. It is not: on the four pool-covered tasks the frozen mean adapter alone (no training) reaches only 0.19 to 0.53 exact match on clean data, while adaptation in the subspace reaches 0.68 to 0.99 (for example wiki_qa 0.44 to 0.99, social_iqa 0.19 to 0.68). The method learns substantially beyond its prior; the prior is part of the method, and we report its standalone score so the improvement is visible. On race, where the pool is weak, the mean adapter and the adapted model are both near the base (0.11 and 0.13), consistent with the plasticity ceiling.

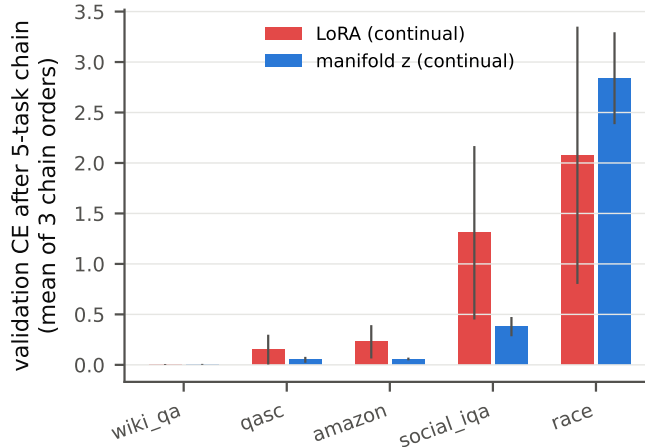


Figure 5: Validation CE on all five tasks after learning them in sequence with a single continually-updated adapter, mean over the three chain orders. On the tasks the pool covers, z forgets less than LoRA; race is the exception.

Table 2: Controls, exact match, mean over 3 seeds. Family holdout removes all 4 to 9 same-dataset adapters from the basis. Random subspace replaces the pool with 128 norm-matched random rank-16 directions.

Task	family holdout		random subspace	
	z clean	z flip100	clean	flip100
wiki_qa	0.99	0.99	0.15	0.03
qasc	0.98	0.94	0.29	0.09
amazon	0.95	0.96	0.53	0.38
social_iqa	0.70	0.65	0.06	0.02

4.8 Adaptive backdoor attack

The attacks so far fail because they lie outside the subspace. The sharper test is an *adaptive* attacker who searches for a harmful behavior expressible *inside* it: a backdoor that maps a trigger token to a target output while preserving clean accuracy. We give the attacker the defense itself, optimizing the code z (and, as baseline, LoRA) directly on triggered data, and we exclude the target’s dataset family from the basis.

The result is not uniform, and the non-uniformity is the finding. Unconstrained LoRA plants the backdoor at will (attack success 0.84 to 1.00 while keeping clean accuracy, 1.00 when pushed maximally). Constrained adaptation blocks it on amazon (ceiling 0.08) but not on social_iqa (ceiling 0.85). The difference is consistent with the same principle as the rest of the paper: the backdoor appears blocked when its target behavior lies outside the pool’s common directions. On amazon the target “output negative regardless of sentiment” contradicts every sentiment adapter, so no z we found expresses it; on social_iqa the task is itself a yes/no validity judgment, “always No” is a frequent pool direction, and the trigger latches onto it. With two tasks we cannot claim a general law, only a plausible and testable one: the security boundary looks pool-relative, and its strength may be anticipated from whether the feared behavior is representable in the pool. This moves a binary claim (“it blocks backdoors”) toward a characterized one (“it blocks backdoors whose target is not already a pool behavior”), which is the more defensible and more useful statement.

5 Limitations and threats to validity

Clean pool assumed. The central assumption is that the adapter pool is trusted. We secure the *adaptation data*, not the pool: an attacker who can inject a malicious adapter into the pool moves the subspace and

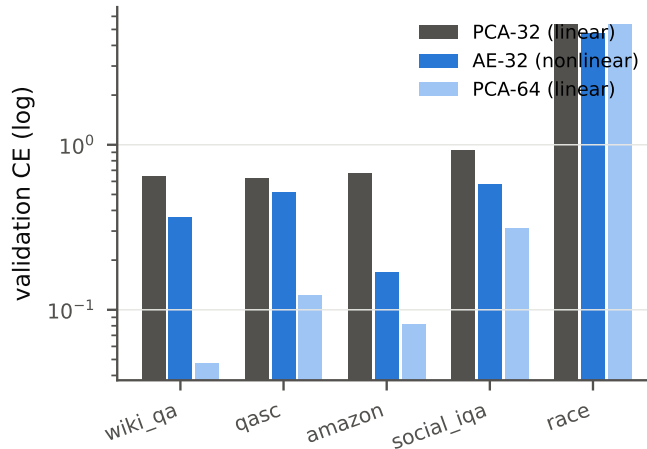


Figure 6: Reconstructing a held-out adapter through a code of fixed size, then evaluating its function. A nonlinear autoencoder at bottleneck 32 (AE-32) beats a linear PCA truncation at 32 components on every task, but a linear PCA at 64 components beats them both.

defeats the protection. Securing the pool is a separate supply-chain problem (provenance, vetting, anomaly detection on the pool spectrum) and is out of scope. **No formal guarantee.** The subspace is spanned by legitimate adapters but is not their convex hull; it contains far extrapolations, negative combinations, and behaviors present in no single adapter, and composed adapters can be unsafe even when each is benign [4]. Our results are empirical protection against the tested attacks, not a proof of behavioral safety. A convex-hull restriction ($g_j \geq 0, \sum_j g_j = 1$) or a trust-region ($z^\top \Sigma^{-1} z \leq \rho$) would bound extrapolation and is future work. **Threat-model breadth.** We test label inversion, garbage targets, and an adaptive trigger backdoor (Section 4.8). The adaptive result bounds the claim honestly: the subspace is a security boundary only against behaviors it does not already contain, and a determined attacker whose target aligns with the pool (social_iqa) partly succeeds. Remaining stronger cases: low-rate backdoors (0.5–5%) that preserve clean accuracy [9], clean-label poisoning, and multi-token or optimized triggers. **Plasticity ceiling.** Performance is capped by pool coverage; on poorly-covered tasks (race) unconstrained fine-tuning wins on clean data. **Scope and baselines.** Single base model, single pool, English P3 tasks, independently trained adapters. Section 4.7 passes four controls (dataset-family holdout, random subspace, strong-regularization LoRA, and a frozen prior baseline). A DoRA variant and EigenLoRAx as a direct comparison remain to be run.

6 Conclusion

Restricting adaptation to a subspace estimated from trusted adapters turns three empirical safety properties into consequences of geometry: the poisoned objectives we test fail to be represented, garbage data announces itself in the loss, and few-shot adaptation is regularized by construction. Concretely, this is the difference between an on-device assistant that can only become a variant of a valid assistant and one that can be steered anywhere, and between a training pipeline that halts on an anomalous-loss spike and one that ships the poison silently. The protection is empirical and bounded, and the adaptive backdoor sharpens the picture: across our tasks the subspace stops an attack when the attack’s target behavior is not already something the pool can do, and lets it through when it is. This is not a weakness of the analysis but its content, since whether a feared behavior is in the pool is something one can check before deployment. What we establish, on the tasks we test, is that a trusted adapter subspace is a restricted-adaptation policy whose poisoning resistance is measurable, tracks pool coverage, and comes with a built-in incompatibility signal.

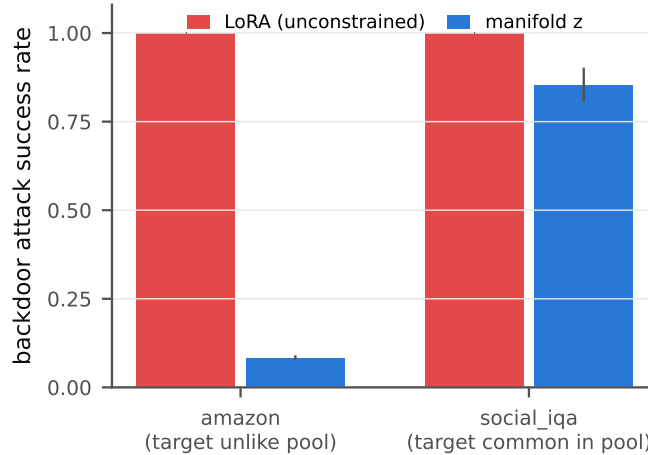


Figure 7: Adaptive backdoor. An attacker inserts a rare trigger token and optimizes (in the maxASR mode, ignoring clean accuracy) to make triggered inputs output a fixed target. Unconstrained LoRA reaches 100% attack success on both tasks. Constrained adaptation caps the attack at 8% when the target behavior is unlike anything in the pool (amazon: force “negative” regardless of sentiment) but only at 85% when the target coincides with a behavior the pool already exhibits (social_iqa, a yes/no validity task where “always No” is a nearby legitimate direction).

7 Reproducibility

All scripts, seeds, and incremental JSON outputs are in the repository. Every experiment runs on one 12 GB GPU in bf16; the spectrum analysis runs on CPU.

References

- [1] Samuel K. Ainsworth, Jonathan Hayase, and Siddhartha Srinivasa. Git re-basin: Merging models modulo permutation symmetries. In *International Conference on Learning Representations*, 2023.
- [2] Rickard Brüel-Gabrielsson, Jiacheng Zhu, Onkar Bhardwaj, Leshem Choshen, Kristjan Greenewald, Mikhail Yurochkin, and Justin Solomon. Compress then serve: Serving thousands of lora adapters with little overhead. *arXiv preprint arXiv:2407.00066*, 2024.
- [3] Rujikorn Charakorn, Edoardo Cetin, Yujin Tang, and Robert Tjarko Lange. Text-to-lora: Instant transformer adaption. In *International Conference on Machine Learning*, 2025. arXiv:2506.06105.
- [4] Sihao Ding et al. Colluding lora: A compositional vulnerability in llm safety alignment. *arXiv preprint arXiv:2603.12681*, 2026.
- [5] Chengsong Huang, Qian Liu, Bill Yuchen Lin, Tianyu Pang, Chao Du, and Min Lin. Lorahub: Efficient cross-task generalization via dynamic lora composition. In *Conference on Language Modeling*, 2024.
- [6] Prakhar Kaushik, Ankit Vaidya, Shravan Chaudhari, and Alan Yuille. Eigenlorax: Recycling adapters to find principal subspaces for resource-efficient adaptation and inference. *arXiv preprint arXiv:2502.04700*, 2025.
- [7] Zhiyuan Liang, Dongwen Tang, Yuhao Zhou, Xuanlei Zhao, Mingjia Shi, Wangbo Zhao, Zekai Li, Peihao Wang, Konstantin Schürholt, Damian Borth, Michael M. Bronstein, Yang You, Zhangyang Wang, and Kai Wang. Drag-and-drop llms: Zero-shot prompt-to-weights. *arXiv preprint arXiv:2506.16406*, 2025.

- [8] Xiangyu Qi, Yi Zeng, Tinghao Xie, Pin-Yu Chen, Ruoxi Jia, Prateek Mittal, and Peter Henderson. Fine-tuning aligned language models compromises safety, even when users do not intend to! In *International Conference on Learning Representations*, 2024.
- [9] Jayaram Raghuram, George Kesidis, and David J. Miller. A study of backdoors in instruction fine-tuned language models. *arXiv preprint arXiv:2406.07778*, 2024.
- [10] Andrei A. Rusu, Dushyant Rao, Jakub Sygnowski, Oriol Vinyals, Razvan Pascanu, Simon Osindero, and Raia Hadsell. Meta-learning with latent embedding optimization. In *International Conference on Learning Representations*, 2019.
- [11] Konstantin Schürholt, Diyar Taskiran, Boris Knyazev, Xavier Giró-i Nieto, and Damian Borth. Model zoos: A dataset of diverse populations of neural network models. In *Advances in Neural Information Processing Systems, Datasets and Benchmarks Track*, 2022.
- [12] Alexander Wan, Eric Wallace, Sheng Shen, and Dan Klein. Poisoning language models during instruction tuning. In *International Conference on Machine Learning*, 2023.